Article

Not peer-reviewed version

Advanced-Glycation End Products-Selective Probe Development

Heewon Cho , Na-Kyeong Hong , Insung Yong , Haw-Young Kwon , Nam-Young Kang , Larissa Miasiro Ciaramicoli , Pilnam Kim , Young-Tae Chang *

Posted Date: 28 February 2024

doi: 10.20944/preprints202402.1624.v1

Keywords: Advanced glycation products; fluorescence small molecule; Fluorescence library; Screening; Aging

 doi:10.20944/preprints202402.1624.v1

Article

Advanced-Glycation End Products-Selective Probe Development

Heewon Cho [1,†], Na-Kyeong Hong [1,†], Insung Yong [2], Haw-Young Kwon [1], Nam-Young Kang [3], Larissa Miasiro Ciaramicoli [1], Pilnam Kim [2] and Young-Tae Chang [1,*]

[1] Department of Chemistry, Pohang University of Science and Technology (POSTECH), Pohang, Gyeongsangbuk-do, 37673, Republic of Korea; heewon@postech.ac.kr; nkhong5868@postech.ac.kr; khy0305@postech.ac.kr; larissaciaramicoli@gmail.com; ytchang@postech.ac.kr

[2] Department of Bio and Brain Engineering, Korea Advanced Institute of Science and Technology (KAIST), Daejeon, 34141, Republic of Korea; aassyt76@kaist.ac.kr; pkim@kaist.ac.kr

[3] Department of Convergence IT Engineering, Pohang University of Science and Technology (POSTECH), Pohang, Gyeongsangbuk-do, 37673, Republic of Korea; knysg@postech.ac.kr

* Correspondence: ytchang@postech.ac.kr

† These authors contributed equally to this work.

Abstract: Advanced glycation end products (AGEs) play a significant role in the aging processes, further regarding as a hallmark of aging. Despite the importance, a lack of monitoring tools has hampered the study of relationship between AGEs and aging. Here, we firstly report a novel AGEs-selective probe, **AGO**. **AGO** presented its ability to detect AGEs more sensitively than a conventional approach of measuring autofluorescence from AGEs. In addition, we confirmed that **AGO** can detect AGEs depending on kinetics, reflecting by a preference to ribose-derived AGEs. Finally, **AGO** revealed its competence to visualize glycation products in glycation mimicking model, made by collagen framework. We believe that this study will enrich molecular toolboxes to understand physiological processes of AGEs during aging processes.

Keywords: advanced glycation products; fluorescence small molecule; fluorescence library; screening; aging

1. Introduction

Advanced glycation end products (AGEs) are a diverse group of compounds formed through a non-enzymatic reaction between reducing sugars and proteins, lipids, or nucleic acids[1]. This reaction, known as glycation or the Maillard reaction, occurs spontaneously under normal physiological conditions[2]. AGEs accumulate over time in various tissues and organs, especially in long-lived proteins like collagen and elastin[3]. In recent times, numerous scientific investigations have shown that AGEs can serve as a hallmark of aging on a molecular scale (Figure 1). The intricate relationship between AGEs and aging is multifaceted. Furthermore, the accumulation of AGEs has been linked to the development of age-related diseases such as diabetes, cardiovascular issues, neurodegenerative disorders, and kidney dysfunction[4]. Consequently, comprehending the complex interplay between AGE accumulation and the aging process bears significant implications for therapeutic strategies aimed at mitigating age-related ailments and fostering healthy aging. Therefore, monitoring AGE levels in biological samples may provide valuable information regarding the progression of age-related conditions. However, the relationship between aging and AGEs has been complicated to be uncovered due to several reasons, including a shortage of available and precise techniques to measure specific AGEs, and a deficiency in AGEs mimicking models that reproduce the conditions[4].

The most common way to detect AGEs is measuring the autofluorescence of AGEs using fluorescence spectroscopy. However, this method lacks specificity and sensitivity and may be influenced by other fluorescent compounds present in biological samples, along with high background, considering excitation by a ultra violet region. Considering the emergence of AGEs as a

 doi:10.20944/preprints202402.1624.v1

potential biomarker, it is necessary to overcome the current limitations and elicit new molecular tools to detect AGEs with high sensitivity.

Fluorescent small molecules have earned significant interest because of their prospective roles in sensor and visualization. Though a conventional approach to probe development typically relies on established molecular recognition processes for specific substances, its efficacy and efficiency within complex biological environments remains inconsistent despite thorough planning. Consequently, the pace and breadth of probe elicitation have been hampered by several inherent constraints. To surmount these challenges, diverse fluorescence library methods have been employed to generate novel fluorescent probes, even in scenarios where prior comprehension of the target recognition mechanism is lacking[5]. Our group has established huge amounts of fluorescence libraries, DOFL (Diversity Oriented Fluorescence Library; >10,000 compounds)[6]. With a systematic approach, we have successfully reported more than 30 fluorescent small molecules applying to various biological samples[7-11]. Here, we firstly developed AGEs-selective probe, **AGO**, through screening DOFL. **AGO** showed the highest selectivity over 2080 compounds, and a better sensitivity to AGEs compared to autofluorescence from AGEs. Moreover, we observed that **AGO** can highly sense ribose-derived glycation products, compared to other hexoses or disaccharide. Finally, the ability of **AGO** was demonstrated in a glycated collagen framework, mimicking the natural glycation of the matrix.

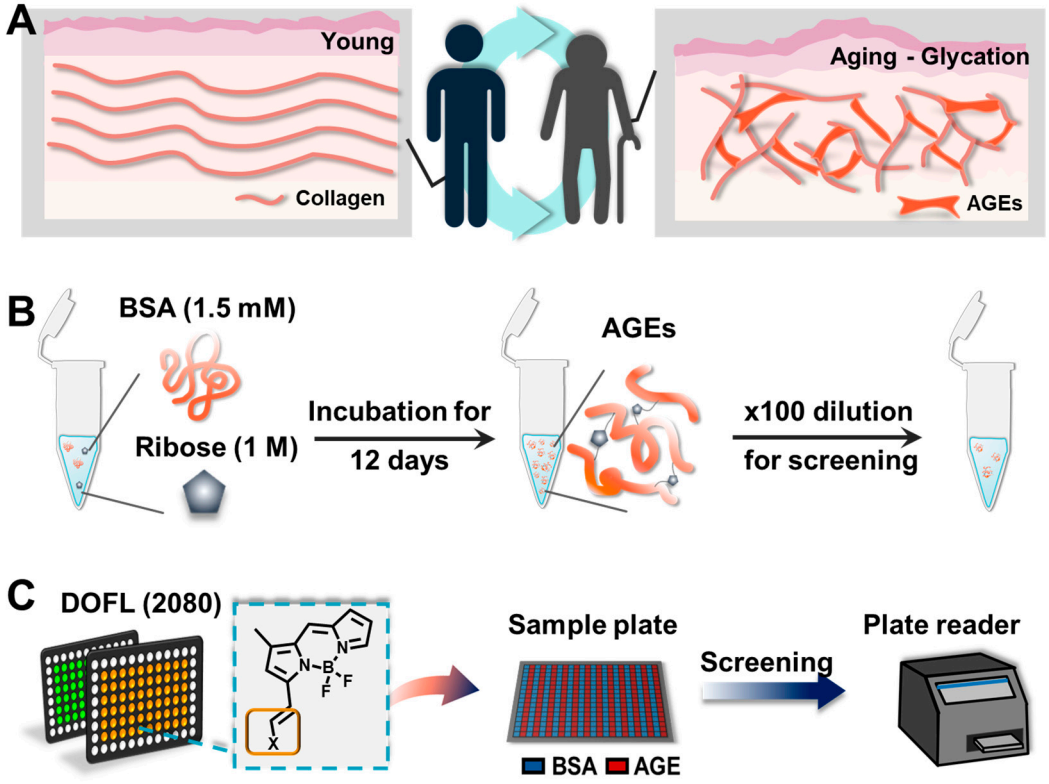

Figure 1. Advanced glycation end products (AGEs) formation process. A) Schematic view of AGE formation during an aging process. It is created with BioRender.com B) Sample preparation of AGEs using BSA. C) Illustration of the screening process.

2. Materials and Methods

2.1. Materials

D-(+)-Galactose (Sigma Aldrich; St. Louis, Mo, USA), D-(+)-Mannose, D-(+)-Ribose, sucrose, and bovine serum albumin were purchased from Sigma Aldrich (St. Louis, Mo, USA). We acquired D-(+)-Glucose from Alfa Aesar (Haverhill, MA, USA), and D-(+)-Xylose from TCI (Tokyo, Japan).

 doi:10.20944/preprints202402.1624.v1

2.2. Glycation of BSA

BSA was dissolved in PBS, containing 0.05% sodium azide to yield a stock solution of 3 mM. This solution was resuspended with carbohydrates, prepared in PBS with 0.05% sodium azide to a final concentration of 1.5 mM BSA and 1 M carbohydrates. The mixtures were incubated at 37°C, and incubation days were dependent on each experiment. Before a resuspension, all solutions were filtered with 0.45 μm, and 0.22 μm membranes (Millipore, USA).

2.3. DOFL screening

26 DOFL library (including 2080 compounds) was used for 384-well based screening. For the screening, compounds (100 μM in DMSO) were mixed with AGE solution to a final concentration of 5 μM compounds. After 30 minutes incubation at room temperature, plates were read by a plate reader (Molecular Devices, USA).

2.4. TEM image

The TEM images were taken by JEOL JEM1011 (JEOL USA, INC, Peabody, MA). BSA stock solution was resuspended with Ribose to a final concentration of 1 M, and incubated at 37°C for 12 days. The concentrations of both stock solutions were used after dilution by a factor of 20x, and images were captured by 150k objective lens. The samples for imaging were prepared followed by instructions.

2.5. Fluorescence microscopy

BSA (1.5 mM) and D-ribose (1 M) were incubated at 37°C until 12 days at the intervals of 2 days. After 12 days, samples were stained with **AGO** (5 μM) for 30 min at room temperature. The samples (50 μL) were transferred to 384-well plate after dilution of stock solution to 100. The fluorescence from solution was taken by fluorescence microscopy using Operetta CLS (Perkin Elmer,Walthan,MA, USA) with x10 objective lens. AGEs autofluorescence was captured by DAPI channel (ex: 355-385 / em: 430-500), and **AGO** fluorescence was measured with TRITC channel (ex: 530-560/570-650). Each channel was set to give 20% power and expose to 10 ms.

2.6. Assay of AGEs derived by different carbohydrate types

The mixtures of BSA (1.5 mM) and each carbohydrate (1 M) including glucose, galactose, mannose, ribose, xylose, and sucrose, were incubated at 37°C until 24 days, and mixtures were prepared at the intervals of 6 days. To conduct the assay, the samples were made after 100x dilution, and transferred them into 96-well plate. The mixtures were measured by the plate reader (Molecular Devices, USA) after staining with **AGO** (5 μM) for 30 min at room temperature. The autofluorescence data was acquired by excitation at 370 nm, and emission at 420 nm. **AGO** graph was obtained by excitation at 490 nm, and emission at 570 nm.

2.7. Preparation of Glycated Collagen Hydrogel

To fabricate collagen microgels, the collagen type I solution (Corning, 354249) was neutralized to a physiological pH (approximately 7.0-7.4) utilizing a mixture comprised of 1N sodium hydroxide (NaOH), distilled water, and 10x phosphate-buffered saline (PBS), conducted on ice as per the manufacturer's instructions. Subsequently, the solution's concentration was meticulously adjusted to 3 mg/mL. Following the neutralization process, 100 μL of the collagen mixture was carefully pipetted into each well of a 24-well plate (SPL, 30024). Gelation was then initiated by incubating the plates at 37°C for 1 h, facilitating the polymerization of the collagen. Upon completion of the gelation process, the resulting hydrogel was immersed in a 500 mM ribose solution (Merck, R9629) prepared in PBS. This was incubated at 37°C for a duration of one week to ensure adequate modification of the hydrogel properties.

 doi:10.20944/preprints202402.1624.v1

2.8. Immunofluorescence staining

After the glycation process, collagen microgels were washed three times with PBS for 10 minutes each to remove any residual ribose. Following this, they were fixed using 4% paraformaldehyde (PFA) for 1 h at room temperature to preserve their microstructures. After fixation, the samples were permeabilized with 0.15% Triton-X 100 in PBS for 30 min. To prevent non-specific antibody binding, the microgels were then blocked with 1% bovine serum albumin (BSA) in PBS for 1 h. Subsequently, they were incubated overnight at 4°C with anti-collagen I (Abcam, ab21286) antibody, followed by a 2-hour incubation with secondary antibodies (Merck, F0382) at room temperature. For a comparison of AGE selectivity in the glycated extracellular matrix (ECM), the hydrogels were stained with 10 μM **AGO**/**AGN** dyes for 1 h. Each step was followed by three 10-minute washes with PBS. Finally, fluorescent images were captured and analyzed using a confocal laser scanning microscope (Nikon, A1R).

2.9. Chemical materials and general methods for AGO synthesis

All used compounds and solvents were purchased from Alfa Aesar (Haverhill, MA, USA), Sigma Aldrich (St. Louis, MO, USA), Combi-Blocks (San Diego, USA), TCI (Tokyo, Japan), and Samchun Chemicals (Seoul, Republic of Korea). All the chemicals were directly used without further purification. MERCK silica gel 60 (230-400 mesh, 0.040-0.063 mm) was used for normal-phase column chromatography. The optical properties were performed with SpectraMax M2e spectrophotometer (Molecular Devices) in 96 well plate (clear bottom) and QS high-precision cuvette. The relative fluorescence quantum yield method was selected, and Rhodamine B (Φ = 0.49) was utilized as the standard. The quantum yield equation was calculated by equation (1). For analytical characterization of AGO HPLC (Agilnet, 1260 series) with a DAD (diode array detector) and a single quadrupole mass spectrometer (Aglient, 6100 series, ESI) were used. Eluents (A: H2O with 0.1% formic acid (FA), B: ACN with 0.1% FA) and Zorbax SB-C18 column (2.1 x 50 mm, 1.8 μm particle size, 80 Å pore size) were used. High-performance liquid chromatography (HPLC) was utilized on Prep. HPLC (Shimadzu) with a PDA detector with a C18(2) Luna column (5 μm, 250 mm × 21.2 mm, 100 Å). A gradient elution of 60% B for 5 min and them, 60% B to 100% B for 40 min, and then 100% B for 55 min was used at flow rate of 8 mL/min (solvent A: H2O; B: ACN). 1H and 13C NMR spectra were obtained from Brucker AVANCE III HD 850.

$$\Phi_{fi} = (F_i/F_s)(f_s/f_i)(n_i/n_s)^2 \bullet \Phi_f^s \quad (1)$$

Where Φ_{fi} and Φ_{fs} represented the fluorescence quantum yield of sample and standard, respectively. F represented the area under curve of the fluorescence spectrum (from 550 to 800 nm), n represented the refractive index of the solvent, and f represented the absorption factor ($f = 1 - 10^{-A}$, where A represented the absorbance) at the excitation wavelength selected for sample and standard.

2.10. Synthesis of AGO

The reaction followed the below procedure. BD (4,4-Difluoro-5,7-dimethyl-4-bora-3a,4a-diaza-S-indacene) (30 mg, 136 μmole), 3-Phenoxybenzaldehyde (32.3 mg, 164 μmole), Acetic acid (47 μL, 818 μmole), Pyrrolidine (69 μL, 818 μmole) were dissolved in ACN (5 mL), stirring at 70°C for 30 min. The collected mixture was concentrated in vacuo. The residue was purified via High-performance liquid chromatography (HPLC) was utilized on Prep. HPLC (Shimadzu) with a PDA detector with a C18(2) Luna column (5 μm, 250 mm × 21.2 mm, 100 Å). A gradient elution of 60% B for 5 min and them, 60% B to 100% B for 40 min, and then 100% B for 55 min was used at flow rate of 8 mL/min (solvent A: H2O; B: ACN). After purification, purple solid was obtained (39.8 mg, 73%). ^{1}H NMR (850 MHz, Chloroform-d) δ 7.71 (s, 1 H), 7.63 (d, J = 16.3 Hz, 1H), 7.43 (d, J = 7.74 Hz, 1H),

7.38 (q, J = 7.65 Hz, 3H), 7.33 (d, J = 16.3 Hz, 1H), 7.28 (s, 1H), 7.24 (t, J = 1.7 Hz), 7.21 (s, 1H), 7.16 (t, J = 7.40 Hz, 1H), 7.06 (d, J = 7.74 Hz, 2H), 7.01 (dd, J = 8.14 Hz, 1H), 6.97 (d, J = 3.83 Hz, 1H), 6.75 (s, 1H), 6.49 (q, J = 3.74 Hz, 3H), 2.33 (s, 3H). ^{13}C NMR (214 MHz, Chloroform-d) δ 158.22, 157.73, 156.95, 144.50, 139.55, 139.01, 137.75, 137.73, 133.30, 130.18, 129.88, 126.48, 123.57, 122.41, 120.09, 119.34, 118.97, 118.51, 117.17, 116.69, 11.51. LC-MS (ESI) $[M+H]^+$, m/z calcd for $C_{24}H_{19}BF_2N_2O$ 400.16, found: 401.0

 doi:10.20944/preprints202402.1624.v1

2.11. Synthesis of AGN

The reaction followed the below procedure. BD (100 mg, 454 μmole), 3-Methoxybenzaldehyde (74.2 mg, 545 μmole), Acetic acid (104 μL, 1820 μmole), Pyrrolidine (152 μL, 1820 μmole) were dissolved in ACN (10 mL), stirring at 70°C for 30 min. The collected mixture was concentrated in vacuo. The residue was purified via High-performance liquid chromatography (HPLC) was utilized on Prep. HPLC (Shimadzu) with a PDA detector with a C18(2) Luna column (5 μm, 250 mm × 21.2 mm, 100 Å). A gradient elution of 60% B for 5 min and them, 60% B to 100% B for 40 min, and then 100% B for 55 min was used at flow rate of 8 mL/min (solvent A: H2O; B: ACN). After purification, purple solid was obtained (33.5 mg, 22 %). 1H NMR (850 MHz, Chloroform-d) δ 7.71 (s, 1 H), 7.63 (d, J = 16.3 Hz, 1H), 7.35 (d, J = 7.74 Hz, 1H), 7.32 (t, J = 7.91 Hz, 1H), 7.28 (s, 1H), 7.22 (d, J = 7.91 Hz), 7.18 (s, 1H), 7.12 (t, J = 1.7 Hz, 1H), 6.95 (d, J = 3.74 Hz, 1H), 6.94(dd, J = 8.14 Hz, 1H), 6.75 (s, 1H), 6.47 (q, J = 3.74 Hz, 3H), 3.88(s, 3H), 2.32 (s, 3H). 13C NMR (214 MHz, Chloroform-d) δ 159.97, 158.61, 144.57, 139.88, 139.14, 137.83, 137.17, 133.21, 129.88, 126.20, 123.33, 120.73, 118.81, 117.24, 116.54, 115.92, 112.68, 55.37, 11.49. LC-MS (ESI) $[M+H]^+$, m/z calcd for $C_{19}H_{17}BF_2N_2O$ 338.14, found: 339.0

2.12. Synthesis of compound G

The reaction followed the below procedure. BD (30 mg, 136 μmole), 2-Phenoxybenzaldehyde (32.3 mg, 164 μmole), Acetic acid (47 μL, 818 μmole), Pyrrolidine (69 μL, 818 μmole) were dissolved in ACN (5 mL), stirring at 70°C for 30 min. The collected mixture was concentrated in vacuo. The residue was purified via High-performance liquid chromatography (HPLC) was utilized on Prep. HPLC (Shimadzu) with a PDA detector with a C18(2) Luna column (5 μm, 250 mm × 21.2 mm, 100 Å). A gradient elution of 60% B for 5 min and them, 60% B to 100% B for 40 min, and then 100% B for 55 min was used at flow rate of 8 mL/min (solvent A: H2O; B: ACN). After purification, purple solid was obtained (11.1 mg, 20%). LC-MS (ESI) $[M+H]^+$, m/z calcd for $C_{24}H_{19}BF_2N_2O$ 400.16, found: 401.

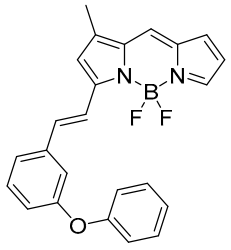

Chemical Formula: $C_{24}H_{19}BF_2N_2O$
Molecular Weight: 400.24
AGO

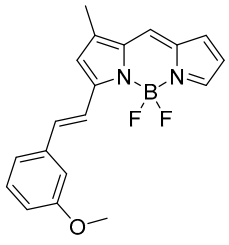

Chemical Formula: $C_{19}H_{17}BF_2N_2O$
Molecular Weight: 338.16
AGN

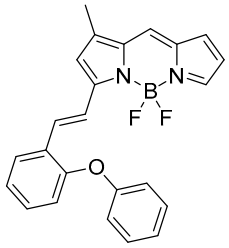

Chemical Formula: $C_{24}H_{19}BF_2N_2O$
Molecular Weight: 400.24
Compound G

3. Results

3.1. Development of AGE selective probe

To elicit an AGE-selective probe, we firstly prepared glycation samples in vitro using bovine serum albumin (BSA), which has been considered as a standard protein to induce glycation, and ribose that has been known to form AGEs rapidly than other monosaccharides[12]. BSA solution was suspended with D-ribose to a final concentration of 1.5 mM BSA and 1 M ribose, and then the mixtures were incubated at 37°C (Figure 1B). After 12 days, we checked whether AGEs were formed using transmission electron microscopy (TEM)[12]. We expected that glycation products may show globular aggregation, resulting in bigger particles than BSA[13]. Compared to BSA, images showed that glycation was clearly generated (Figure S1). Then, we prepared a systematic screening system (Figure 1C). First, we carefully set potential fluorescence libraries from DOFL that can target AGEs with a higher chance. We selected Boron dipyrromethene (BODIPY)-including libraries, composed of 2080 compounds, as BODIPY is a highly lipophilic neutral fluorophore[14], implying AGEs-friendly molecules. Then, we added BSA and AGE samples in 384-well plates, and they were incubated with BODIPY compounds (5 μM) for 30 min. After reading the plates with a plate reader,

 doi:10.20944/preprints202402.1624.v1

we narrowed down the results having complete emission wavelength shapes, and then analyzed AGE selectivity by calculating fluorescence intensity of AGE divided by BSA. The numeric values were plotted to one-dimensional graph (Figure 2A). We found that one compound showed the highest selectivity to AGE over BSA (~6 fold), and dubbed it as **AGO** (Advanced Glycation end products Orange) (Figure 2B). **AGO** consisted of BODIPY fluorophore with a meta-positioned phenoxybenzyl ring. To scrutinize a structural preference to AGE, we unfolded three molecular compositions taking up over 4-fold selectivity to AGE compared to BSA (Figure 2E-F). Interestingly, one compound had phenoxybenzyl derivative in a para location (Figure 2F), also belonging to **AGO**. Since we supposed that this moiety may give a particular ability to sense AGEs, we newly synthesized a BODIPY compound including ortho positioned phenoxybenzyl ring that was not contained in DOFL (Figure 2G). Though the molecule can discriminate AGE over BSA, its capability was not superior to **AGO**. Moreover, we confirmed that methoxybenzyl moiety cannot distinguish between AGE and BSA, and called it as **AGN** (Advanced Glycation end products Negative) (Figure 2C). Therefore, we concluded that phenoxybenzyl derivative with a proper attachment would bring a high capacity to sense AGE.

Preprints.org (www.preprints.org) | NOT PEER-REVIEWED | Posted: 28 February 2024 doi:10.20944/preprints202402.1624.v1

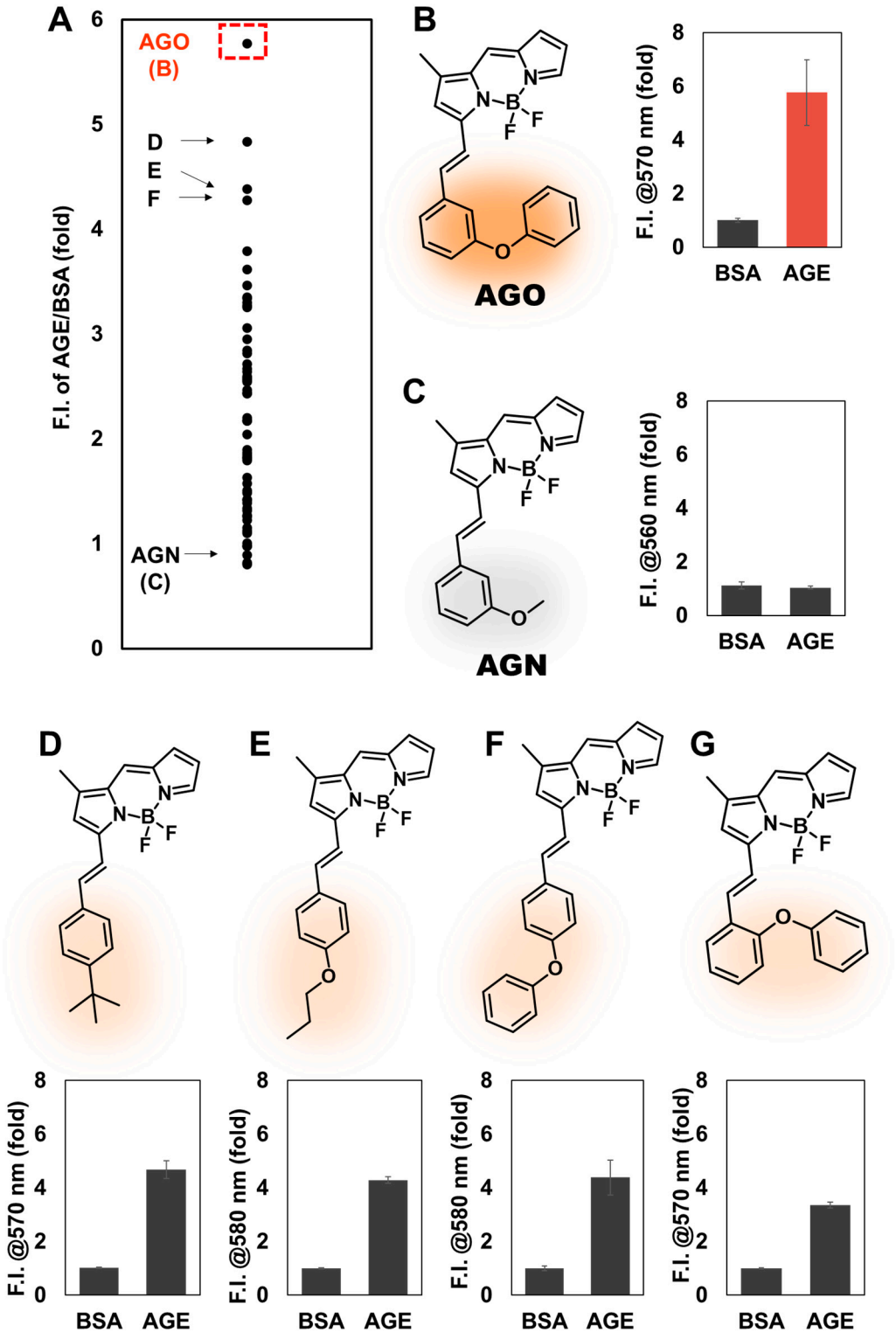

Figure 2. Development of AGE selective sensor. A) Analyzed results are plotted into one-dimensional graph. B) The most promising candidate, AGO. B) Negative control compound's structure and result. D-G) Candidates' structures selective to AGE and their results.

3.2. Development of AGE selective probe

Inspired by the selectivity of **AGO**, we wanted to test whether **AGO** can systematically detect AGEs. We first prepared AGE samples, derived by incubating BSA and ribose, in a day-dependent manner at the intervals of 2 days until 12 days. The formation of AGEs was measured by its

 doi:10.20944/preprints202402.1624.v1

autofluorescence using the plate reader (Ex: 370 nm; Em: 420 nm) (Figure 3A). The signal was continuously increased, but it was saturated after 8 days. On the other hand, **AGO** invariably kept its AGEs-sensing ability until 12 days (Figure 3B). Moreover, we next checked its selectivity using fluorescence microscopy for its wide application. As similar with the previous result, while autofluorescence was escalated by 8 days by setting its limitation (Figure 3C), **AGO** continuously can sense AGEs (Figure 3D). In addition, the displayed images revealed that discriminating AGEs over BSA is more sensitive and selective when using **AGO**, compared to autofluorescence measurement.

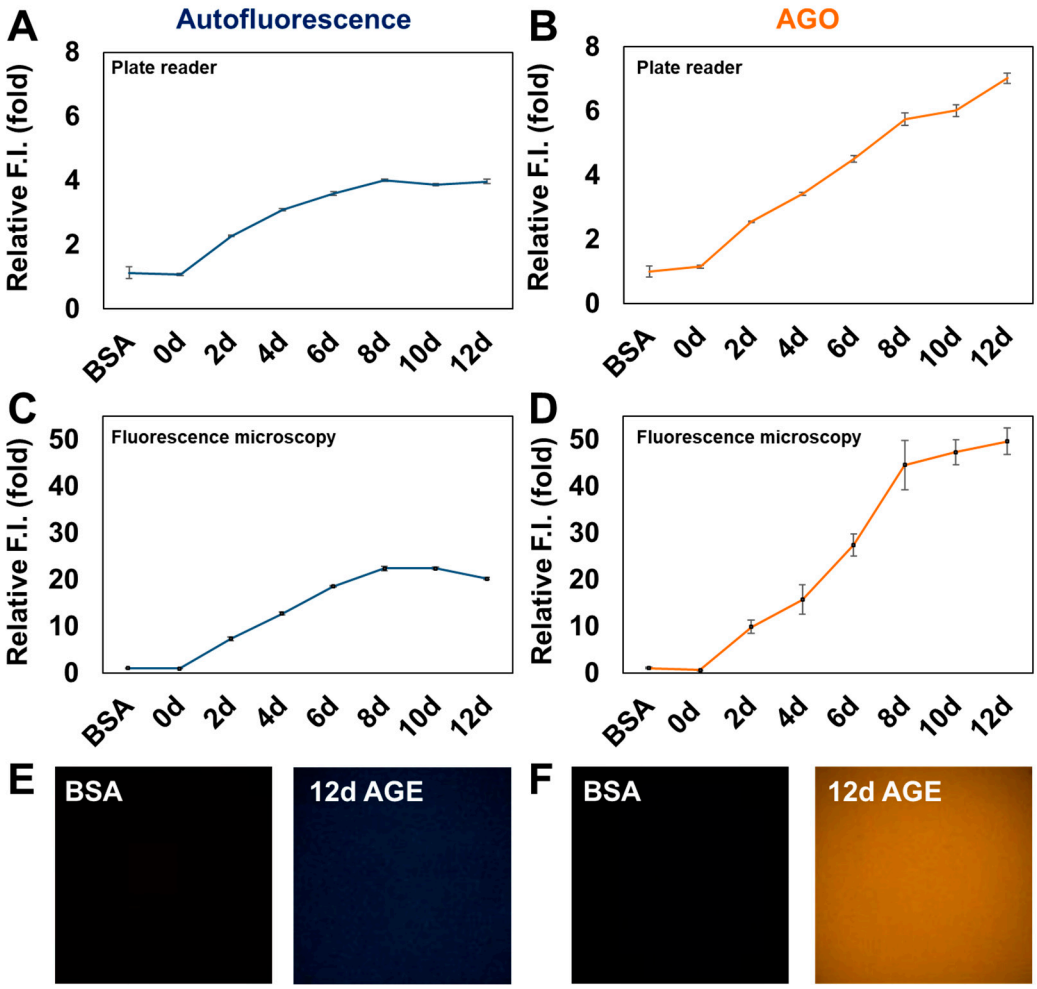

Figure 3. AGO showed higher selectivity to day-dependent AGE than the autofluorescence of AGE itself. A) Autofluorescence of AGEs, and B) AGO intensity were measured by plate reader. C) Autofluorescence and D) AGO intensity were assessed by fluorescence microscopy. The corresponding images of E) autofluorescence, and F) AGO fluorescence were displayed.

3.3. AGO sensitivity to AGEs derived by different types of carbohydrates

Next, we wondered how **AGO** behaves in AGEs made by different carbohydrate types. We prepared three pyranoses (glucose, galactose and mannose), two furanoses (ribose, and xylose), and sucrose, which is a disaccharide formed by fructose and glucose. It has been reported that each carbohydrate may need a different period to reach to maximum yields of AGEs [15-17], we lengthened incubation time until 24 days. Then, we measured autofluorescence to check whether AGEs have been formed properly. Interestingly, the autofluorescence of ribose, incubated with BSA, recorded top rapidly at 6 days compared to other saccharides (Figure S2). This observation was in line with previous research that ribose has higher ability to generate AGEs than other carbohydrate types[12,16]. In addition to ribose, xylose and galactose showed their capacity to form AGEs, but it seemed to be difficult to keep up with the record of ribose. Based on this observation, we realized that pentose has quicker kinetics than hexose. It could be explained by the ratio of opened form

 doi:10.20944/preprints202402.1624.v1

(aldehyde) existed 5-fold higher in pentose (around 0.1%) than hexose (~0.02%)[18]. In addition, unequal competence may be derived by a structural stability, as a pentose ring can generate an unstable aldofuranose, described as "puckered", which is vulnerable to react with amino acids[19]. It was reflected by **AGO**, which preferred to detect pentose-derived AGEs, particularly in ribose (Figure 4). Based on these results, **AGO** revealed sensitively detecting skill of AGEs generated by furanoses, especially ribose, superior to AGEs autofluorescence.

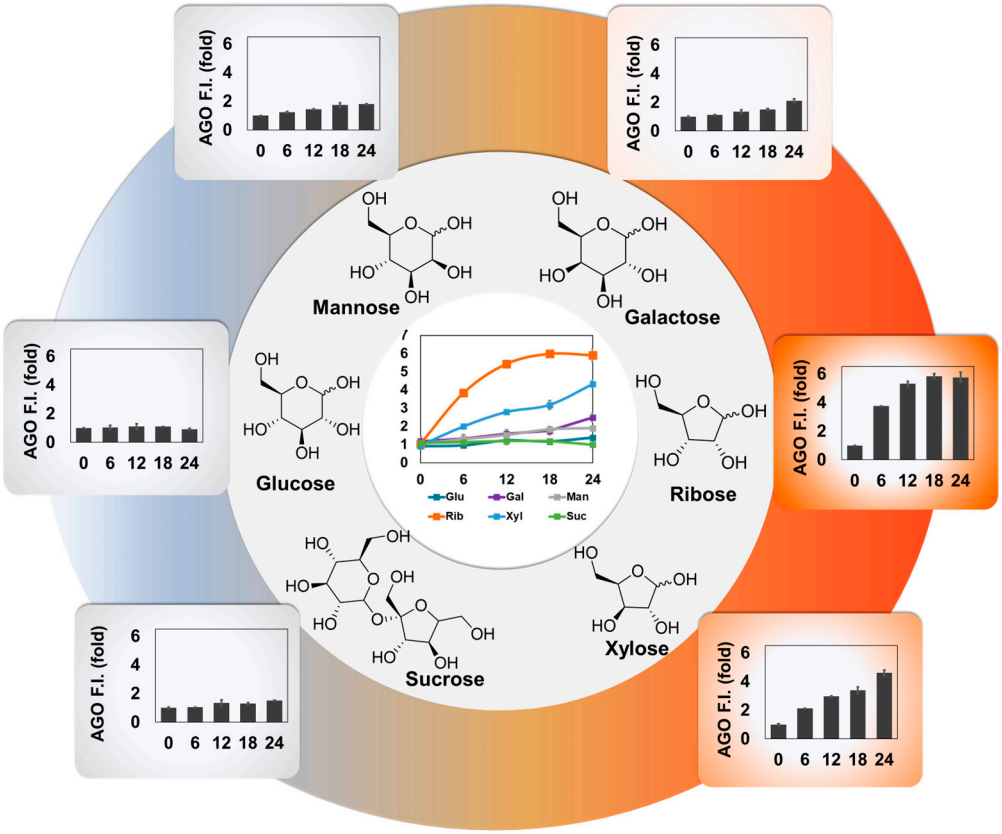

Figure 4. AGO selectivity to carbohydrate type-dependent AGEs formation. AGEs were formed by glucose, galactose, mannose, ribose, xylose and sucrose incubated with BSA until 24 days at the intervals of 6 days. Relative fluorescence intensity of AGO was plotted in bar graphs.

3.4. AGO se lectivity in a glycation mimicing model

To deeply explore the selectivity of **AGO**, we created a glycated collagen framework, mimicking the natural glycation of the matrix. Collagen presents a susceptible target for glycation product formation due to several factors: 1) Its prevalence as one of the most abundant proteins in the human body[20]; 2) Collagen has an extended half-life, increasing the probability of exposure to sugars[21]; 3) Its distinctive triple helical configuration consisting of lengthy amino acid chains, facilitating multiple sugar-binding sites and rendering it conducive to glycation[20]; 4) The presence of lysine residues in collagen, which are particularly prone to glycation reactions[22]. For these reasons, we posited that collagen could serve as a representative model for glycation environments, showcasing biochemically induced AGE formation and heightened stiffness along with disrupted ECM structure. Firstly, a collagen solution underwent pre-glycation with D-ribose. The alterations in the mechanical and structural characteristics of the glycated matrix have been investigated in a previous work. The study verified non-enzymatic glycated collagen framework, characterized by elongated, reinforced, and extensively crosslinked collagen fibers[23]. After the glycation process, collagen microgels were added with 10 μM of **AGO**, and also prepared **AGN** (negatively control) stained-samples together to clearly validate the selectivity of **AGO**, after staining with anti-collagen I. Compared to **AGN** that had a lack of ability to detect AGEs (Figure 5A), the images obviously proved that **AGO** can stain AGEs (Figure 5B), which fluorescence was overlapped with the signal of collagen antibody. This

 doi:10.20944/preprints202402.1624.v1

result indicated the competence of **AGO** to selectively sense AGEs even in glycation mimicking model.

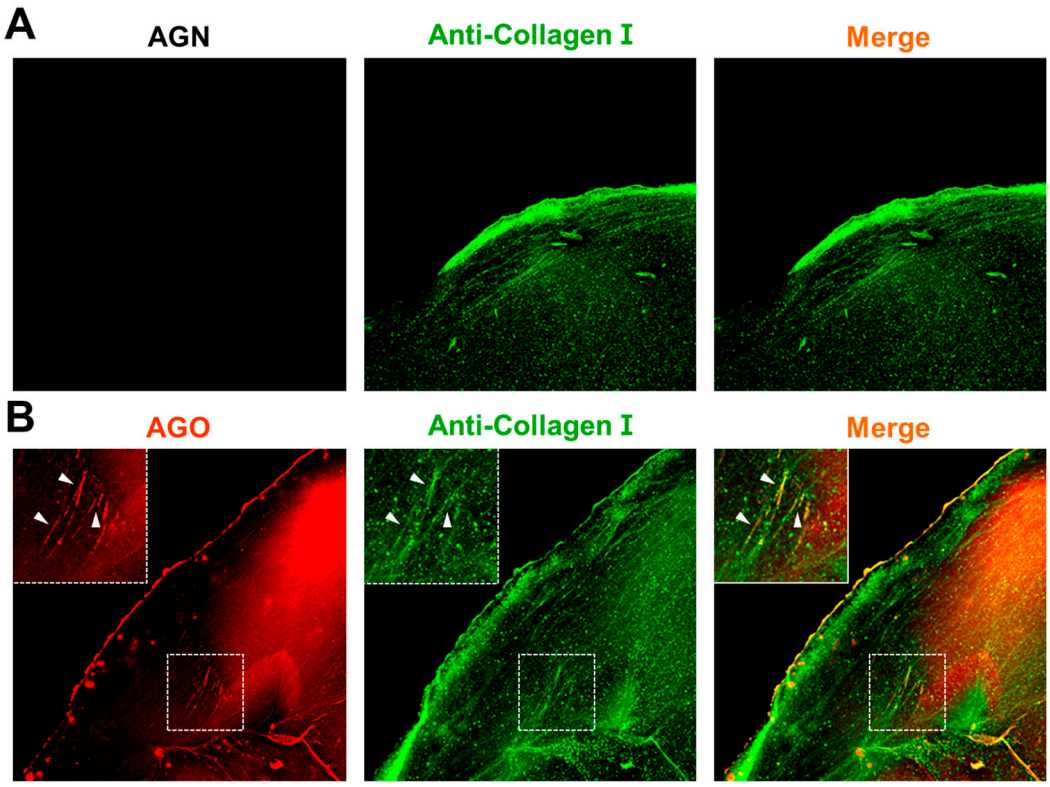

Figure 5. AGO selectivity to AGE derived from collagen model. The generated AGEs were stained by A) AGN and B) AGO.

4. Discussion

Aging, an intricate biological process, encompasses a myriad of molecular and cellular changes over time, influencing various physiological functions. Among the multitude of factors implicated in the aging process, the accumulation of advanced glycation end products (AGEs) has emerged as a significant contributor. Despite its importance, the relationship between aging and AGEs has not been well established yet. One of the major factors contributing to this gap is the lack of competent monitoring tools. The most common method involves detecting AGEs using autofluorescence. However, autofluorescence typically occurs at shorter wavelengths (~420 nm), resulting in high background levels and the possibility of detecting other biological molecules in complex systems. Therefore, there is a need to develop an efficient molecular tool for sensing AGEs.

To develop such a probe, we selected BODIPY-fluorescence libraries from DOFL, considering the lipophilic characteristics of BODIPY that may enhance the opportunity to detect AGEs. We then prepared AGEs using BSA and ribose, confirming their formation by TEM. After screening samples with fluorescence molecules, we identified one molecule that exhibited the highest selectivity among 2080 compounds. It comprised a BODIPY fluorophore with a meta-positioned phenoxybenzene moiety. Through structure-activity relationship studies, we concluded that phenoxybenzene, along with its proper positioning, enables sensitive detection of AGEs.

Furthermore, we compared the selectivity of AGE detection between autofluorescence and **AGO** fluorescence. Interestingly, autofluorescence could detect AGEs adequately but reached its limit at a certain point. In contrast, **AGO** exhibited continuous and sensitive detection of AGEs over time. The efficacy of **AGO** was further validated using fluorescence microscopy, where **AGO** demonstrated a much more vivid sensing ability compared to autofluorescence under similar conditions. This indicates the potential of **AGO** to replace autofluorescence for measuring AGEs more meticulously.

 doi:10.20944/preprints202402.1624.v1

Motivated by the sensitivity of **AGO**, we investigated how **AGO** behaves in AGEs derived from different types of carbohydrates. We prepared three hexoses (glucose, galactose, mannose), two furanoses (ribose, xylose), and one disaccharide (composed of glucose and fructose), incubating each sugar with BSA. Interestingly, ribose exhibited a higher glycation effect than other sources, followed by xylose and galactose. Based on this observation, we speculate that aging processes may be accelerated by certain carbohydrate sources. This phenomenon was also observed with **AGO**, implying that **AGO** can systematically measure the kinetics of AGE formation.

Finally, we confirmed the selectivity of **AGO** in a glycated collagen model, mimicking natural phenomena. Collagen, the most abundant protein in the human body[20], constitutes a significant portion of connective tissues such as skin[24] or tendons[25]. It provides structural support, elasticity, and strength to various tissues. However, once collagen is glycated, physiological processes may be disrupted due to the accumulation of glycation products[3]. AGEs can cross-link with collagen fibers, resulting in the formation of rigid and dysfunctional collagen structures. Additionally, collagen cross-linking by AGEs increases tissue stiffness and disrupts cell-matrix interactions[26]. Overall, the accumulation of AGEs and their interactions with collagen can have detrimental effects on tissue structure and function, particularly in aging processes. Taking into account the impacts of AGEs on collagen during aging processes, our results indicate a notable progression in comprehending the role of AGEs in aging. Moreover, they indicate the potential for AGO as an effective diagnostic tool for detecting AGEs in vitro.

5. Conclusion

In this manuscript, to the best of our knowledge, we firstly reported AGEs-selective probe, **AGO**. **AGO** revealed its capability to sensitive detection AGEs compared to the autofluorescence from AGEs. Moreover, **AGO** can highly sense pentose-derived AGEs, especially ribose, among heterogenous populations of AGEs. Also, we proved that **AGO** selectively visualize AGEs in AGEs environmental mimicking collagen model.

Supplementary Materials: The following supporting information can be downloaded at the website of this paper posted on Preprints.org.

Author Contributions: Conceptualization, H.Cho, N.-K.Hong, H.-Y.Kwon, N.-Y.Kang, L.M.C, and Y.-T.Chang; methodology, H.Cho, N.-K.Hong, I.Yong, L.M.C, P.Kim, and Y.-T.Chang; software, H.Cho, and N.-K.Hong; validation, H.Cho, N.-K.Hong, and I.Yong; investigation, H.Cho, N.-K.Hong, I.Yong, H.-Y.Kwon, N.-Y.Kang, L.M.C, P.Kim, and Y.-T.Chang; data curation, H.Cho, and N.-K.Hong; writing—original draft preparation, H.Cho.; writing—review and editing, Y.-T.Chang.; visualization, H.Cho, N-K.Hong, I.Yong.; supervision, Y.-T.Chang.; project administration, Y.-T.Cahng.; funding acquisition, H.-Y.Kwon, N.-Y.Kang, Y.-T.Chang. All authors have read and agreed to the published version of the manuscript.

Funding: This research was supported by Basic Science Research Institute Fund (2021R1A6A1A10042944 to Y.-T.C), the National Research Foundation of Korea (NRF) grant funded by the Korea government (MSIT) (2023R1A2C300453411 to Y.-T. C), the National Research Foundation of Korea (NRF) grant funded by the Korea government (MSIT) (2020R1A2C2009776 to N.-Y. K; RS-2023-00210972 to H.-Y.K), and the Ministry of Education (2020R1A6A1A03047902 to N.-Y.K.). H.C. is grateful for financial support from Hyundai Motor Chung Mong-Koo foundation.

Institutional Review Board Statement: Not applicable.

Informed Consent Statement: Not applicable.

Data Availability Statement: The data presented in this study are available on request from the first author (H.Cho).

Conflicts of Interest: The authors declare no conflicts of interest.

References

1. Singh, R.; Barden, A.; Mori, T.; Beilin, L. Advanced glycation end-products: a review. *Diabetologia* **2001**, *44*, 129-146, doi:10.1007/s001250051591.
2. Gkogkolou, P.; Bohm, M. Advanced glycation end products: Key players in skin aging? *Dermatoendocrinol* **2012**, *4*, 259-270, doi:10.4161/derm.22028.

3. Paul, R.G.; Bailey, A.J. Glycation of collagen: the basis of its central role in the late complications of ageing and diabetes. *Int J Biochem Cell Biol* **1996**, *28*, 1297-1310, doi:10.1016/s1357-2725(96)00079-9.
4. Chaudhuri, J.; Bains, Y.; Guha, S.; Kahn, A.; Hall, D.; Bose, N.; Gugliucci, A.; Kapahi, P. The Role of Advanced Glycation End Products in Aging and Metabolic Diseases: Bridging Association and Causality. *Cell Metab* **2018**, *28*, 337-352, doi:10.1016/j.cmet.2018.08.014.
5. Lee, J.S.; Kim, Y.K.; Vendrell, M.; Chang, Y.T. Diversity-oriented fluorescence library approach for the discovery of sensors and probes. *Mol Biosyst* **2009**, *5*, 411-421, doi:10.1039/b821766c.
6. Yun, S.W.; Kang, N.Y.; Park, S.J.; Ha, H.H.; Kim, Y.K.; Lee, J.S.; Chang, Y.T. Diversity oriented fluorescence library approach (DOFLA) for live cell imaging probe development. *Acc Chem Res* **2014**, *47*, 1277-1286, doi:10.1021/ar400285f.
7. Choi, Y.K.; Kim, J.J.; Chang, Y.T. Holding-Oriented versus Gating-Oriented Live-Cell Distinction: Highlighting the Role of Transporters in Cell Imaging Probe Development. *Acc Chem Res* **2019**, *52*, 3097-3107, doi:10.1021/acs.accounts.9b00253.
8. Liu, X.; Chang, Y.T. Fluorescent probe strategy for live cell distinction. *Chem Soc Rev* **2022**, *51*, 1573-1591, doi:10.1039/d1cs00388g.
9. Lee, H.G.; Hong, N.K.; Chang, Y.T. NMN sensor cocktail: selective sensing of nicotinamide mononucleotide over citric acid. *Chem Commun (Camb)* **2023**, *59*, 9372-9375, doi:10.1039/d3cc02501b.
10. Xu, W.; Ren, C.; Teoh, C.L.; Peng, J.; Gadre, S.H.; Rhee, H.W.; Lee, C.L.; Chang, Y.T. An artificial tongue fluorescent sensor array for identification and quantitation of various heavy metal ions. *Anal Chem* **2014**, *86*, 8763-8769, doi:10.1021/ac501953z.
11. Xu, W.; Bai, J.; Peng, J.; Samanta, A.; Divyanshu; Chang, Y.T. Milk quality control: instant and quantitative milk fat determination with a BODIPY sensor-based fluorescence detector. *Chem Commun (Camb)* **2014**, *50*, 10398-10401, doi:10.1039/c4cc04670f.
12. Wei, Y.; Chen, L.; Chen, J.; Ge, L.; He, R.Q. Rapid glycation with D-ribose induces globular amyloid-like aggregations of BSA with high cytotoxicity to SH-SY5Y cells. *BMC Cell Biol* **2009**, *10*, 10, doi:10.1186/1471-2121-10-10.
13. Dasgupta, M.; Kishore, N. Selective inhibition of aggregation/fibrillation of bovine serum albumin by osmolytes: Mechanistic and energetics insights. *PLoS One* **2017**, *12*, e0172208, doi:10.1371/journal.pone.0172208.
14. Wang, J.; Guo, X.; Li, L.; Qiu, H.; Zhang, Z.; Wang, Y.; Sun, G. Application of the Fluorescent Dye BODIPY in the Study of Lipid Dynamics of the Rice Blast Fungus Magnaporthe oryzae. *Molecules* **2018**, *23*, doi:10.3390/molecules23071594.
15. Shen, C.Y.; Wu, C.H.; Lu, C.H.; Kuo, Y.M.; Li, K.J.; Hsieh, S.C.; Yu, C.L. Advanced Glycation End Products of Bovine Serum Albumin Suppressed Th1/Th2 Cytokine but Enhanced Monocyte IL-6 Gene Expression via MAPK-ERK and MyD88 Transduced NF-kappaB p50 Signaling Pathways. *Molecules* **2019**, *24*, doi:10.3390/molecules24132461.
16. Syrovy, I. Glycation of albumin: reaction with glucose, fructose, galactose, ribose or glyceraldehyde measured using four methods. *J Biochem Biophys Methods* **1994**, *28*, 115-121, doi:10.1016/0165-022x(94)90025-6.
17. Lee, J.M.; Veres, S.P. Advanced glycation end-product cross-linking inhibits biomechanical plasticity and characteristic failure morphology of native tendon. *J Appl Physiol (1985)* **2019**, *126*, 832-841, doi:10.1152/japplphysiol.00430.2018.
18. Zhu, Y.; Zajicek, J.; Serianni, A.S. Acyclic forms of [1-(13)C]aldohexoses in aqueous solution: quantitation by (13)C NMR and deuterium isotope effects on tautomeric equilibria. *J Org Chem* **2001**, *66*, 6244-6251, doi:10.1021/jo010541m.
19. Wei, Y.; Han, C.S.; Zhou, J.; Liu, Y.; Chen, L.; He, R.Q. D-ribose in glycation and protein aggregation. *Biochim Biophys Acta* **2012**, *1820*, 488-494, doi:10.1016/j.bbagen.2012.01.005.
20. Ricard-Blum, S. The collagen family. *Cold Spring Harb Perspect Biol* **2011**, *3*, a004978, doi:10.1101/cshperspect.a004978.
21. Verzijl, N.; DeGroot, J.; Thorpe, S.R.; Bank, R.A.; Shaw, J.N.; Lyons, T.J.; Bijlsma, J.W.; Lafeber, F.P.; Baynes, J.W.; TeKoppele, J.M. Effect of collagen turnover on the accumulation of advanced glycation end products. *J Biol Chem* **2000**, *275*, 39027-39031, doi:10.1074/jbc.M006700200.
22. Yamauchi, M.; Sricholpech, M. Lysine post-translational modifications of collagen. *Essays Biochem* **2012**, *52*, 113-133, doi:10.1042/bse0520113.
23. Jang, M.; Oh, S.W.; Lee, Y.; Kim, J.Y.; Ji, E.S.; Kim, P. Targeting extracellular matrix glycation to attenuate fibroblast activation. *Acta Biomater* **2022**, *141*, 255-263, doi:10.1016/j.actbio.2022.01.040.
24. Al-Atif, H. Collagen Supplements for Aging and Wrinkles: A Paradigm Shift in the Fields of Dermatology and Cosmetics. *Dermatol Pract Concept* **2022**, *12*, e2022018, doi:10.5826/dpc.1201a18.

 doi:10.20944/preprints202402.1624.v1

25. Buckley, M.R.; Evans, E.B.; Matuszewski, P.E.; Chen, Y.L.; Satchel, L.N.; Elliott, D.M.; Soslowsky, L.J.; Dodge, G.R. Distributions of types I, II and III collagen by region in the human supraspinatus tendon. *Connect Tissue Res* **2013**, *54*, 374-379, doi:10.3109/03008207.2013.847096.
26. Hoy, R.C.; D'Erminio, D.N.; Krishnamoorthy, D.; Natelson, D.M.; Laudier, D.M.; Illien-Junger, S.; Iatridis, J.C. Advanced glycation end products cause RAGE-dependent annulus fibrosus collagen disruption and loss identified using in situ second harmonic generation imaging in mice intervertebral disk in vivo and in organ culture models. *JOR Spine* **2020**, *3*, e1126, doi:10.1002/jsp2.1126.